

## Inverse scattering problem and the off-shell $T$ matrix

R. J. W. Hodgson\*

*Department of Physics and Astronomy, University of Maryland, College Park, Maryland 20742*

(Received 7 September 1977)

The Marchenko approach to the inverse scattering problem is utilized to generate the half-off-shell transition amplitude from the experimental  $^1S_0$   $n$ - $p$  phase-shift data. The numerical procedures are tested for two potential models, and the real symmetric function  $\sigma(p, k)$  is obtained.

[NUCLEAR REACTIONS Inverse scattering theory, off-shell  $T$  matrix from  $^1S_0$   $n$ - $p$  data.]

### I. INTRODUCTION

In recent years interest has grown concerning the usefulness of the two-body transition amplitude or  $T$  matrix as a convenient device to use in nuclear structure calculations. Investigations in the many-body problem rely on a knowledge of the  $T$  matrix. It is quite straightforward to perform calculations of the properties of nuclear matter or of finite nuclei, once one has knowledge of the complete  $T$  matrix. The usual procedure followed to acquire this knowledge is to employ a two-nucleon potential model. Since whatever potential model one assumes automatically defines the off-shell form of the transition amplitude, interest has developed in finding ways of circumventing the construction of a potential, and instead starting directly from a  $T$  matrix.<sup>1-9</sup> The reader is referred to an excellent review<sup>10</sup> of the subject area of the  $T$  matrix in order to get an idea of the extensive work done to date.

Baranger and collaborators<sup>1</sup> demonstrated how much information in the two-body  $T$  matrix was free to be varied. The unitarity constraint restricts considerably the form that it can take. However, one is able to start from a real symmetric function  $\sigma(k, k')$  of the scattering momenta, and from this function generate the full  $T$  matrix. The diagonal elements of  $\sigma$  are determined in any particular eigenchannel by the scattering phase shift  $\delta_l(k)$ . The off-diagonal elements are then apparently free to be varied according to whatever model one chooses. Sauer<sup>6</sup> presented a number of parametric forms for  $\sigma$ , and examined various constraints which would limit the freedom of variation. This work has also been extended to include the effects of bound states,<sup>2</sup> and of coupled channels.<sup>6</sup>

Alternative techniques have also been developed which use the two-body scattering data to directly derive the half-shell  $T$  matrix.<sup>8,9</sup> Some of these have been pursued to the point of doing nuclear

calculations.<sup>6,11</sup> It would of course be desirable if one could build up a model of the  $\sigma$  function directly from field-theoretic information. An approach along these lines by Reiner<sup>9</sup> proves quite promising. However, at present the approach is somewhat restricted by its complexity, and by a number of uncertainties such as the coupling constants, form factors, etc.

An unattractive feature of the  $\sigma$  function is that it is far removed from physical quantities, and if it is to be useful one needs to incorporate as far as possible, sound physical information into its form. It is well known for example that if one assumes a local, energy-independent potential, a knowledge of the phase shift at all energies [i.e.,  $\sigma(k, k)$  for all  $k$ ] in the absence of bound states uniquely determines the potential and hence  $\sigma(p, k)$ . Any variations from this  $\sigma(p, k)$  would arise from differing degrees of nonlocality in the underlying interaction. It would thus appear to be an attractive starting point to have a knowledge of  $\sigma(p, k)$  for a purely local interaction. This approach also has the advantage that one can separately vary the high-energy form of the phase shift, and the degree of nonlocality.

A number of methods have been proposed in the literature for carrying out the potential inversion problem.<sup>12-14</sup> Some are much more amenable to numerical calculations than others. Karlsson<sup>14</sup> has recently outlined procedures which can very nicely enable one to generate half-off-shell  $T$  matrices from a knowledge of the on-shell data. With such an approach it is for example possible to generate a  $\sigma(p, k)$  function to use in the method of Baranger *et al.*,<sup>1</sup> or, more importantly, to use as a starting point in examining the effects of introducing nonlocal variations in  $\sigma$ , and of varying the form of the high-energy phase shift. One can then, at least for some partial wave states, separate the local and nonlocal effects.

We have utilized the approach of Karlsson<sup>14</sup> to examine the utility of such a scheme. In Sec. II

we briefly review the theory behind the Marchenko approach to generating the off-shell transition amplitude, and then illustrate the numerical accuracy of such an approach in Sec. III. Section IV goes on to illustrate what one finds if one uses the experimental  $^1S_0$   $n$ - $p$  phase shift data, and briefly looks at the sensitivity of  $\sigma$  to the high-energy phase shift.

## II. BACKGROUND

An approach whereby the half-off-shell partial-wave transition amplitude can be derived from the on-shell amplitude by means of a momentum-space formulation of the Marchenko integral equation has recently been presented by Karlsson.<sup>14</sup> The main ideas of this approach are summarized in this section.

The on-shell amplitude or  $T$  matrix for a given partial wave is specified in terms of the real phase shift  $\delta_l(k)$ ,

$$t_l(k, k; E + i\epsilon) = -\frac{2}{\pi k} \sin \delta_l(k) e^{i\delta_l(k)}, \quad (2.1)$$

in units such that  $\hbar^2 = 2m = 1$ , and with  $E = k^2$ . The properties of this amplitude also enable one to express the half-shell amplitude  $t_l(p, k; E + i\epsilon)$  in terms of a real function  $f_l(p, k)$ ,

$$t_l(p, k; E + i\epsilon) = f_l(p, k) t_l(k, k; E + i\epsilon), \quad (2.2)$$

$$f_l(p, k) = (p/k)^l + (p^2 - k^2) \frac{k}{\sin \delta_l(k)} \int_0^\infty r dr \int_r^\infty r' dr' j_l(pr) A_l(r, r') \operatorname{Im}[h_l^{(+)}(kr') e^{i\delta_l(k)}]. \quad (2.5)$$

Introducing a second solution to the Schrödinger equation,  $h_l^{R(\pm)}(k; r)$ , which also satisfies the boundary conditions (2.4), but which is associated with the potential

$$v_l(r) = \frac{l(l+1)}{r^2} \theta(R-r), \quad (2.6)$$

one can express  $f_l^{(\pm)}$  in terms of this function through another Volterra kernel  $B$ ,

$$f_l^{(\pm)}(k; r') = h_l^{R(\pm)}(k; r') + \frac{1}{r'} \int_{r'}^\infty r'' dr'' B_l(r', r'') h_l^{R(\pm)}(k; r''). \quad (2.7)$$

The function  $\theta(x)$  is the familiar Heaviside step function.

The function  $f_l(p, k)$  can now be related to  $B_l$  in a fashion analogous to (2.5):

$$f_l(p, k) = (p/k)^l + (p^2 - k^2) \frac{k}{\sin \delta_l(k)} \left( \int_0^R r^2 dr \operatorname{Im}[j_l(pr) [h_l^{R(+)}(k; r) - h_l^{(+)}(kr)] e^{i\delta_l(k)}] + \int_0^\infty r dr \int_r^\infty r' dr' j_l(pr) B_l(r, r') \operatorname{Im}[h_l^{R(+)}(k; r') e^{i\delta_l(k)}] \right), \quad (2.8)$$

The half-shell function  $f_l$  is independent of  $R$ , as the kernel  $B$  is a function of  $R$ .

The regular solutions of Schrödinger's equation must necessarily satisfy a completeness relation. In terms of operators, this completeness relation takes the form

so that  $f_l(p, k)$  together with  $\delta_l(k)$  completely specify the half-off-shell amplitude. A knowledge of this half-shell  $T$  matrix is sufficient to obtain the complete off-shell amplitude from the Low equation.<sup>15</sup>

In the inverse scattering theory the Marchenko integral equation relates the solution  $f_l^{(\pm)}(k; r)$  of the partial-wave radial Schrödinger equation to the free-particle solutions  $h_l^{(\pm)}(kr)$  through the kernel  $A_l(r', r)$ :

$$f_l^{(\pm)}(k; r') = h_l^{(\pm)}(kr') + \frac{1}{r'} \int_{r'}^\infty r'' dr'' A_l(r', r'') h_l^{(\pm)}(kr''). \quad (2.3)$$

The solutions  $f_l^{(\pm)}$  satisfy the boundary conditions at infinity,

$$\lim_{r \rightarrow \infty} \frac{f_l^{(\pm)}(k; r)}{h_l^{(\pm)}(kr)} = 1. \quad (2.4)$$

By also employing the out-going-wave scattering solution to the Schrödinger equation, together with its momentum-space transform, the half-shell function  $f_l(p, k)$  can be expressed in terms of  $A_l(r, r')$  and  $h_l^{(\pm)}(kr)$ ,

$$(1+B)(1-F)(1+B^\dagger) = 1, \quad (2.9)$$

where the kernel of the operator  $F$  is given by

$$\frac{1}{rr'} F_l(r', r) = \frac{1}{\pi} \int_0^\infty k^2 dk \operatorname{Re}[h_l^{R(+)}(k; r') h_l^{R(+)}(k; r) \times (e^{2i\delta_l(k)} - 1)], \quad (2.10)$$

for the case where there is no bound state. One can then show that

$$B_i^*(r', r) \theta(r' - r) = F_i(r', r) + \int_r^\infty dr'' F_i(r', r'') B_i^*(r'', r), \quad r' > r, \quad (2.11)$$

which is a linear integral equation for  $B_i^*(r', r)$  in terms of  $F_i(r', r)$ .

The half-shell function  $f_i(p, k)$  can then be computed from (2.8) by substituting into it the iterative solution for  $B_i^*$  from (2.11) and interchanging the order of integration so that all the  $r$  integrations are performed before the  $k$  integrations in the  $F_i(r', r)$  factors.

In the case of the  $l=0$  partial wave with no bound state,

$$F_0(r', r) = \frac{1}{\pi} \int_0^\infty dk \operatorname{Re} [e^{ik(r'+r)} (e^{2i\delta_0(k)} - 1)]. \quad (2.12)$$

Substitution of this into the series obtained from (2.8) yields a compact series for  $f_0(p, k)$ :

$$f_0(p, k) = 1 + (p^2 - k^2) \frac{1}{4 \sin \delta_0(k)} \times \sum_{n=1}^\infty \frac{\Delta_n(k, \frac{1}{2}(k+p)) - \Delta_n(k, \frac{1}{2}(k-p))}{p}, \quad (2.13)$$

$$\Delta_1(k, q) = -\frac{1}{\pi} P \int_{-\infty}^\infty dq' \frac{\sin[\delta_0(k) + \delta_0(q' - q)]}{q'(k + q' - q)} \sin \delta_0(q' - q) + \frac{\sin[\delta_0(k) - \delta_0(q)]}{k - q} \cos \delta_0(q). \quad (3.1)$$

The principal-value part in turn can be regularized by adding and subtracting a term with  $q'=0$ . This integral can then be written in the form

$$-\frac{1}{\pi} \int_a^\infty dy \left[ \frac{\sin[\delta_0(k) + \delta_0(y - q)] \sin \delta_0(y - q)}{y(k + y - q)} + \frac{\sin[\delta_0(k) - \delta_0(y + q)] \sin \delta_0(y + q)}{y(k - y - q)} \right], \quad (3.2)$$

$$-\frac{1}{\pi} \int_{-a}^a \frac{dy}{y} \left[ \frac{\sin[\delta_0(k) + \delta_0(y - q)] \sin \delta_0(y - q)}{(k + y - q)} - \frac{\sin[\delta_0(k) + \delta_0(-q)] \sin \delta_0(-q)}{(k - q)} \right].$$

The cutoff point  $a$  is arbitrary. We find that by using 48-point Gaussian quadrature for the finite-range integral with  $a = 1.5 \text{ fm}^{-1}$  and 24-point Gaussian quadrature for the infinite-range integral, very accurate results can be achieved. For the latter integral, the transformation

$$y_j = a + \tan[\frac{1}{4}\pi(1 \pm x_j)] \quad (3.3)$$

was used, with the  $x_j$  representing the Gaussian points. 24-point Gaussian quadrature was also used to evaluate  $\Delta_n$  for  $n > 1$  together with four-point interpolation to evaluate the required  $\Delta_{n-1}$  values.<sup>17</sup> Since the  $\Delta$  functions are symmetric,  $\Delta_n(-k, -q) = \Delta_n(k, q)$ , all the required values could

where

$$\Delta_n(k, q) = -\frac{1}{\pi} \int_{-\infty}^\infty dq^n \frac{\sin[\delta_0(k) + \delta_0(q^n)]}{k + q^n} \times \Delta_{n-1}(q^n, q^n + q), \quad (2.14)$$

$$\Delta_1(k, q) = -\frac{1}{\pi} \int_{-\infty}^\infty \frac{\sin[\delta_0(k) + \delta_0(q')]}{k + q'} \times \operatorname{Im} \left( e^{i\delta_0(q')} \frac{1}{q + q' + i\epsilon} \right). \quad (2.15)$$

These expressions will be used to perform the numerical calculations discussed in the next sections.

### III. NUMERICAL CHECK

We have tested the numerical accuracy of the technique used to evaluate the preceding  $S$ -state equations by applying it to two potentials: an unbound square-well potential and a three-term Bargmann potential originally proposed by Sprung and Srivastava.<sup>16</sup>

The first-order function  $\Delta_1(k, q)$  needs to be evaluated carefully due to the singularity at  $q' + q = 0$  and the rapid variation of the integrand in the neighborhood of  $q' = 0$ . By first shifting the singularity to the origin the integration can be expressed in terms of a principal-value integral,

be stored in a  $24 \times 48$  dimensional array.

The square well potential chosen is defined by

$$V_0 = 17.84 \text{ MeV}, \quad 0 < r < R, \quad (3.4)$$

$$= 0, \quad r > R,$$

with  $R = 2.306 \text{ fm}$ . For this potential the off-shell Jost function<sup>18</sup> for the  $l$ th partial-wave state is given by

$$\mathcal{L}(k, q) = (q/K)^l C_l + \frac{k^2 - q^2}{K^2 - q^2}, \quad (3.5)$$

with  $K^2 = V_0 + k^2$ . Here

$$B_l = -\frac{V_0}{(K^2 - q^2)K} W[u_l(Ka), w_l^{(+)}(qa)], \quad (3.6)$$

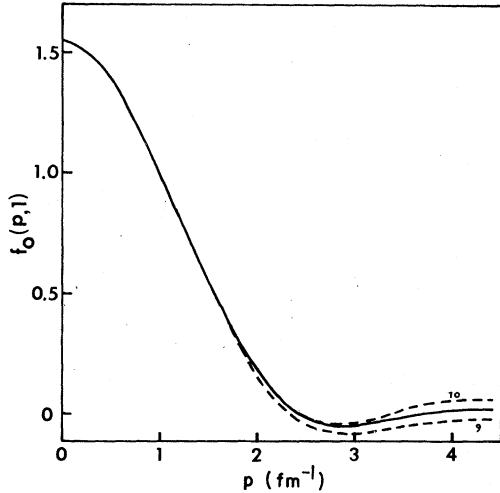


FIG. 1. The half-shell function  $f_0(p, k)$  for  $k=1.0 \text{ fm}^{-1}$  obtained from the square-well phase shift. The two dashed curves represent the series approximation for  $n=9$  and  $n=10$ . The solid curve is the exact result.

with  $u_l(z) = z j_l(z)$  and  $w_l^{(+)}(z) = z h_l^{(+)}(z)$ . The phase shift for  $l=0$  is given by

$$\delta_0(k) = \tan^{-1}\left(\frac{k}{K} \tan Ka\right) - ka. \quad (3.7)$$

The off-shell Jost function is related to the half-shell transition amplitude according to

$$t_l(k, q; E + i\epsilon) = (k/q)^l \frac{\mathcal{L}(k, q) - \mathcal{L}(k, -q)}{\pi i q \mathcal{L}(k)}. \quad (3.8)$$

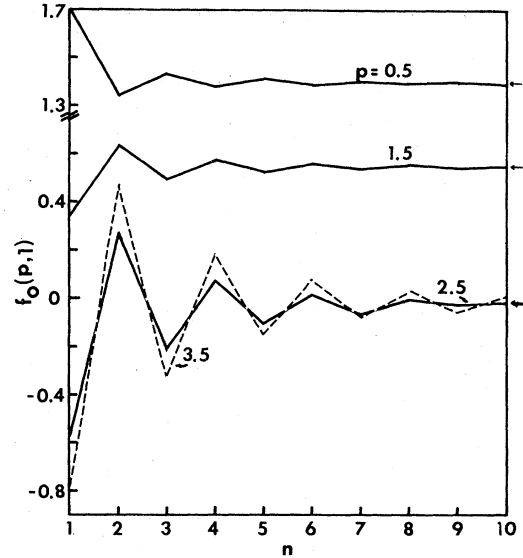


FIG. 2. Convergence of  $f_0(p, k)$  for  $k=1.0 \text{ fm}^{-1}$  as a function of  $n$ , the number of terms included. The arrows indicate the exact results for various  $p$  values. Square-well case. Note the change of scale on the ordinate axis.

The half-shell function  $f_0(p, k)$  was computed using (2.13)–(2.15) including terms up to tenth order. For small  $p$  and  $k$  values (less than  $1.5 \text{ fm}^{-1}$ ) the results are almost indistinguishable from the exact results. Figure 1 illustrates how the series for  $f_0(p, 1.0)$  converges to the exact result for large

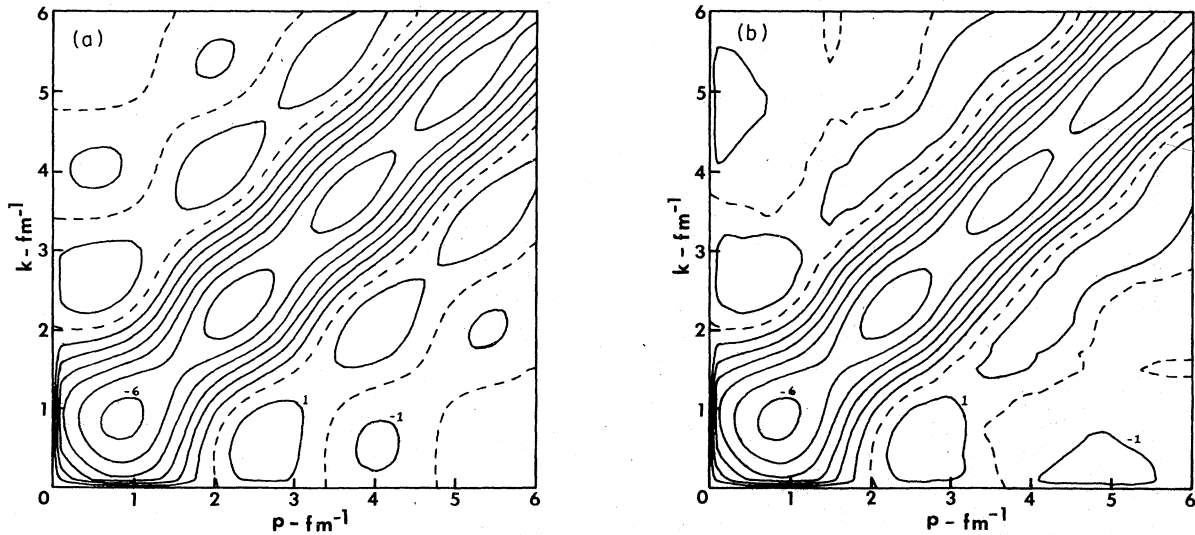


FIG. 3. Contour plots of  $\sigma(p, k)$  computed for the square-well potential. The contours are drawn in steps of  $0.05$  with the dashed curves representing the  $\sigma=0$  contours. The label  $m$  on a contour indicates that it is the  $\sigma=m \times 0.05$  contour. (a) The exact  $\sigma(p, k)$  case. (b) The approximation to  $\sigma(p, k)$  found by averaging the ninth- and tenth-order summations.

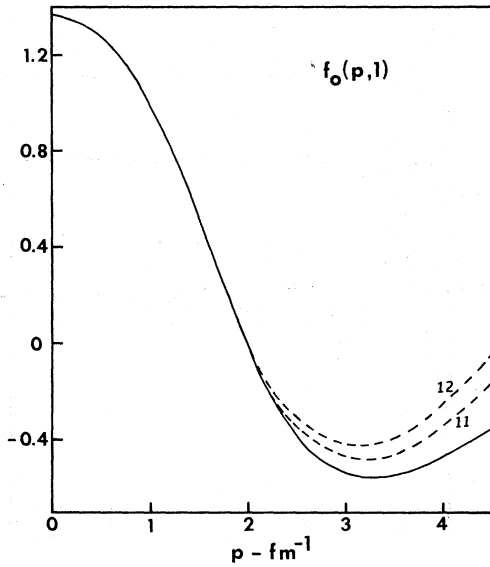


FIG. 4. The half-shell function  $f_0(p, k)$  for  $k = 1.0 \text{ fm}^{-1}$  obtained from the Bargmann phase shift. The dashed curves represent the series approximations for  $n = 11$  and  $n = 12$ . The solid curve is the exact result.

$p$  and  $k$  values. This behavior is amplified further in Fig. 2, where values of  $f_0(p, 1.0)$  are shown as a function of the number of terms summed in the series (2.13). One nice feature that appears in this case is the oscillation of the sum about the exact result. This enables one to extrapolate the results without having to go to large  $n$  values. Although various techniques may be used to do this, we have found that by simply averaging the last two orders we obtained a very good estimate

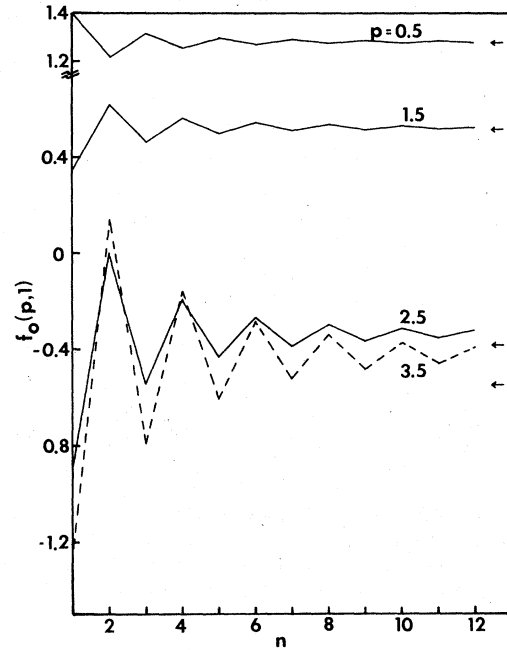


FIG. 5. Convergence of  $f_0(p, 1.0)$  as a function of  $n$  for the Bargmann phase shift. See the caption for Fig. 2.

of the exact result. This averaging approach was used to compute the symmetric function of Baranger, *et al.*,<sup>1</sup>

$$\sigma(p, k) = -\frac{1}{\pi} [kf_0(k, p) \sin \delta_0(p) + pf_0(p, k) \sin \delta_0(k)]. \quad (3.9)$$

That is, at each point, the average of the ninth-

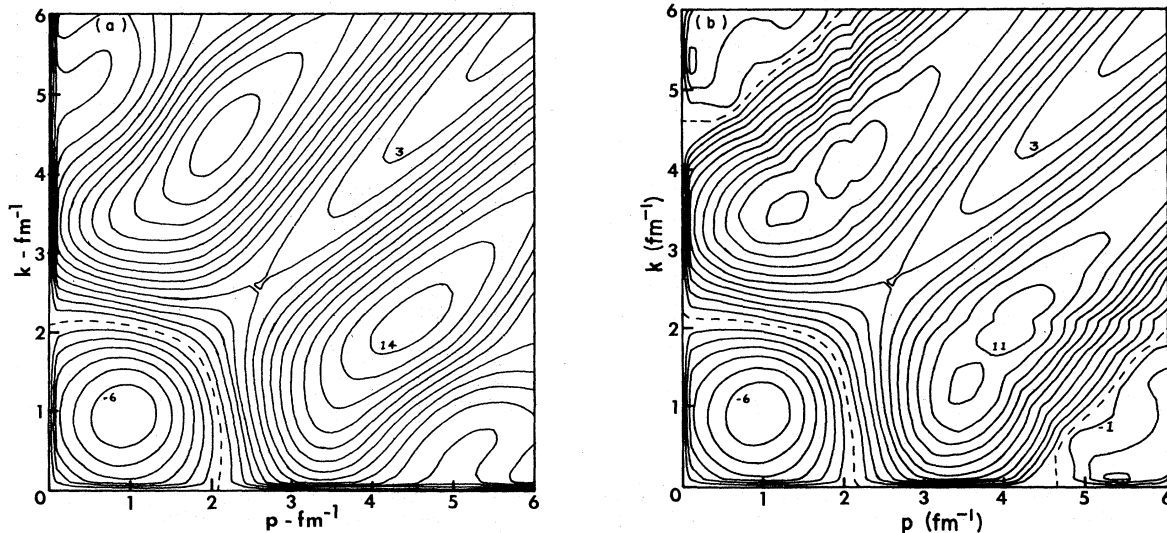


FIG. 6. Contour plots of  $\sigma(p, k)$  computed from the Bargmann potential. See Fig. 3 for explanation. (a) The exact case. (b) The approximate  $\sigma(p, k)$  contours found by averaging the  $n = 11$  and  $n = 12$  results.

and tenth-order sums was taken. The resulting contour plots of the exact and approximate results are displayed in Fig. 3. Each plot was constructed from a  $60 \times 60$  mesh of  $\sigma(p, k)$  values.

The contour plots within the rectangular region  $p \lesssim 2.5 \text{ fm}^{-1}$ ,  $k \lesssim 2.5 \text{ fm}^{-1}$  are virtually identical. As one goes to larger  $p, k$  values, the distance away from the diagonal line  $p = k$  within which agreement is good, tends to decrease.

The Bargmann potential is defined in terms of the  $S$  matrix:

$$S(k) = e^{2i\delta_0(k)} = \prod_{r=1}^3 \frac{k + i\beta_r}{k - i\beta_r} \frac{k - i\alpha_r}{k + i\alpha_r}, \quad (3.10)$$

which can incorporate the change of sign of the phase shift in the  $^1S_0$  state with the proper choice of parameters. Sprung and Srivastava<sup>16</sup> performed a least-squares fit to the  $\delta(^1S_0)$  values of  $n$ - $p$  scat-

$$f_0(p, k) = 1 + (p^2 - k^2) \frac{1}{p \sin \delta_0(k)} \sum_{i=1}^3 \text{Im} \left( e^{i\delta_0(k)} \frac{i}{k + i\beta_i} \int_0^\infty dr M_i(r) e^{-\beta_i r} e^{ikr} \sin pr \right). \quad (3.12)$$

Notice that here  $f_0(p, k)$  has a singularity when  $\delta_0(k) = 0$ . The function  $\sigma(p, k)$ , however, has no such singularity.

In this case, due to the change of sign of  $\delta_0(k)$ , numerical accuracy was more difficult to achieve. In evaluating the integrals (3.2) in  $\Delta_1(k, q)$  we used  $a = 0.5 \text{ fm}^{-1}$ , and also split the first integral into a finite-range part ( $0.5$ – $1.0 \text{ fm}^{-1}$ ) and an infinite-range part. 48-point Gaussian integration was used for all finite-range integrals, together with 24-point Gaussian integration for the infinite-range part. Here, for large  $p$  and  $k$  values, the series again converged in an oscillating manner, but not to the exact result. This is shown in Fig. 4 where the series approximations to  $f_0(p, 1.0)$  are presented for  $n = 11$  and  $12$ , and are compared with the exact result obtained using (3.12). The agreement for small  $p$  is still very good, however, the numerical inaccuracies arising from the quadrature procedure used tend to amplify the error for large  $p$  values. Trial runs made using more integration points did decrease the discrepancy, but at the cost of considerably increased computing time. It was felt that the additional cost was unwarranted at this time, until other methods of obtaining  $f_0(p, k)$ , as will be mentioned later, have been pursued.

The rate of convergence for the series with the Bargmann phase shift was found to be very similar to that of the square-well phase shift. This is shown in Fig. 5. The  $\sigma(p, k)$  contours were also plotted for this case in Fig. 6. The approximate results were obtained by averaging the eleventh- and twelfth-order sums. As in the square-well

tering of MacGregor, Arndt, and Wright<sup>19</sup> yielding a  $\chi^2$  of 12.2. The resulting parameters are

$$\begin{aligned} \alpha_1 &= 0.0404, \\ \alpha_{2,3} &= 1.2192 \pm i1.8918, \\ \beta_1 &= 0.8788, \\ \beta_{2,3} &= 0.8000 \pm i1.5659. \end{aligned}$$

We have used this phase shift to generate the  $\Delta_n$  functions and to compute  $f_0(p, k)$ . Expressions for the exact result have been given by Sprung and Srivastava<sup>16</sup>:

$$B_0^\dagger(r', r) = \sum_{i=1}^3 M_i(r) e^{-\beta_i r'}, \quad (3.11)$$

where  $M_i(r)$  are given in Eq. (7) of their paper. It is then straightforward to show that

case, the differences in the region of small  $p$  and  $k$  ( $\lesssim 2.5 \text{ fm}^{-1}$ ) are quite small. Beyond this region, and away from the region bordering the diagonal ( $|p - k| \approx 1.0 \text{ fm}^{-1}$ ) the discrepancies are larger than in the square-well case.

#### IV. EXPERIMENTAL PHASE SHIFT

We have next taken the experimental  $^1S_0$   $n$ - $p$  phase shift as deduced by MacGregor, Arndt, and Wright,<sup>19</sup> extrapolated this to higher energies, and used the result as the  $\delta_0(k)$  phase shift required for the generation of the  $\Delta_n$  series. Interpolation between the experimental data points has been achieved by using a rational-fraction<sup>20</sup> fitting procedure. Extrapolation is achieved by then matching this with a smooth continuous function,<sup>21</sup>

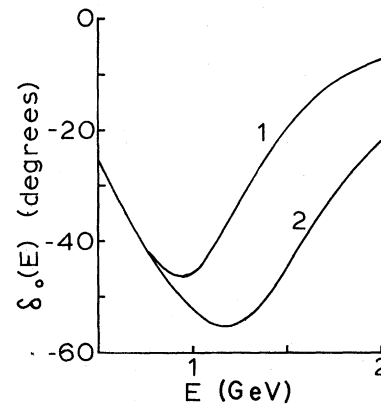


FIG. 7. The high-energy forms of the  $^1S_0$  phase shift.

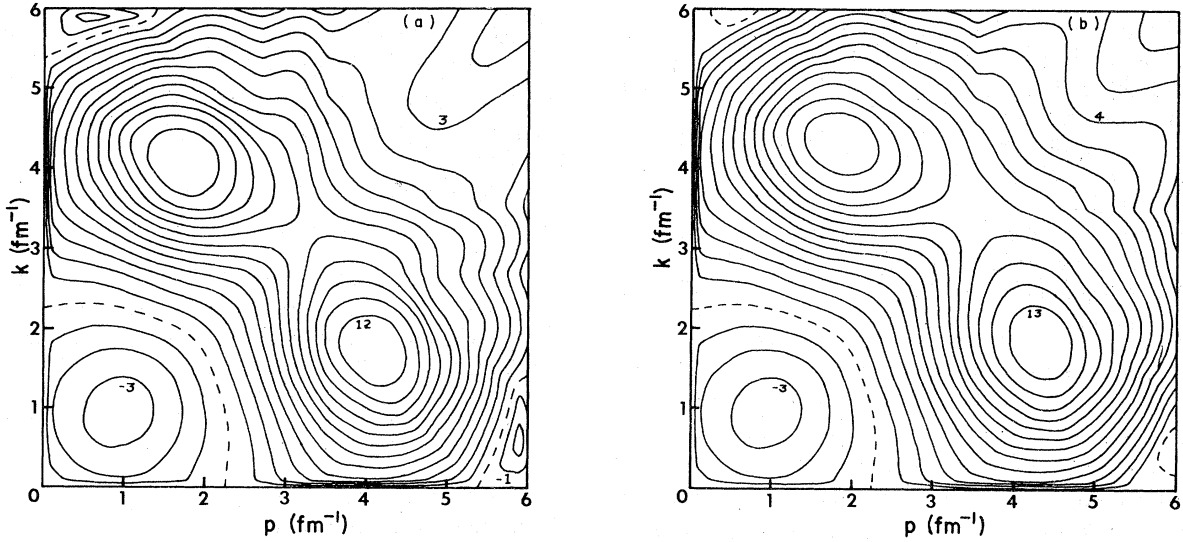


FIG. 8. Contour plots of  $\sigma(p, k)$  as computed from the experimental  $n-p$  phase shift data. The contours are drawn in steps of 0.1 after averaging the eleventh- and twelfth-order results. (a) For high-energy form No. 1; (b) for high-energy form No. 2.

$$\delta(k) = [\delta_0(k_c) + C(k - k_c)] e^{-\alpha(k - k_c)} / [1 + m(k - k_c)^n]. \quad (4.1)$$

The matching point occurs at  $k = k_c$  and  $C$  is determined by the value of  $d\delta_0(k)/dk$  at  $k = k_c$ . Two different forms have been examined with the corresponding high-energy phase shift shown in Fig. 7.

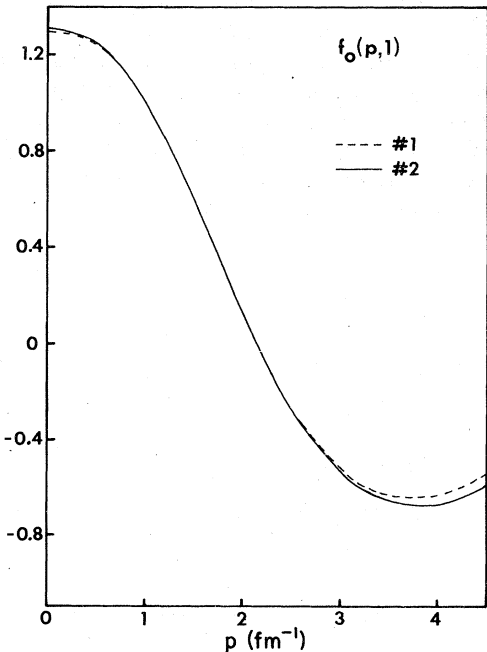


FIG. 9. The half-shell function  $f_0(p, 1.0)$  for the two experimental sets of phase shifts.

The parameters for set No. 1 are  $\alpha = 0.01$ ,  $m = 0.5$ ,  $n = 4$ , and  $E_c = 600$  MeV ( $E_c$  is the energy corresponding to  $k_c$ ). The corresponding parameters for set No. 2 are  $\alpha = 0.01$ ,  $m = 0.2$ ,  $n = 4$ , and  $E_c = 700$  MeV.

The resulting  $\sigma(p, k)$  contours are displayed in Fig. 8. As expected, the change in the high-energy form of  $\delta_0(k)$  leaves the behavior of  $\sigma$  in the region  $p, k \lesssim 3.0$  fm $^{-1}$  virtually unaffected. It has been shown elsewhere<sup>6</sup> that this part of  $\sigma$  dominates in the calculation of the properties of finite nuclei and nuclear matter. It is essentially determined by the known part of  $\delta_0(k)$ . We also show in Fig. 9 the form of  $f_0(p, k)$  with  $k = 1.0$  fm $^{-1}$ . As with the  $\sigma(p, k)$  contours, these have been obtained by averaging the eleventh- and twelfth-order summations. The rate of convergence of the series in this case is very similar to that shown in Fig. 5 for the Bargmann case.

## V. DISCUSSION

We have shown that the approach outlined in Sec. II can be used to generate the half-shell  $T$  matrix from a knowledge of the partial-wave phase shift  $\delta_l(k)$ . The theory is based on the assumption that the underlying potential is local and energy independent. Specifically we have treated the  $^1S_0$  partial-wave case and have found that the resulting  $f_0(p, k)$  or  $\sigma(p, k)$  values are fairly reliable in the region  $p$  or  $k \lesssim 2.5$  fm $^{-1}$ . The approximations made in performing the integrations introduce errors which are enhanced at larger  $p$  or  $k$  values, away from the diagonal. Results from the square-well

potential studied indicate that this should not be as much of a problem in higher partial waves, where the phase shift does not change sign.

A knowledge of  $\sigma(p, k)$ , or equivalently  $f_0(p, k)$ , can be the starting point for performing a number of calculations.<sup>10</sup> Many nuclear structure calculations do not appear to be sensitive to the region beyond  $p$  or  $k$  values of 2.5-3.0 fm<sup>-1</sup>,<sup>6</sup> so that the numerical approach here can still be useful. One can also use the  $\sigma(p, k)$  functions generated by this approach as a starting point for examining the effects of nonlocal variations introduced through unitary transformations.

The  $\Delta_n$  series used to calculate  $f_l(p, k)$  is not

unique, and in many cases may not even be convergent. Karlsson<sup>14</sup> has outlined alternative series expansions for the half-shell amplitude which are always convergent, even in the case where the potential supports a bound state. These have yet to be investigated in detail to study their suitability for applications. Work has been initiated in this area.

The author wishes to acknowledge the generous support of the University of Maryland Computer Science Center. This work was also supported in part by the National Research Council of Canada and the U.S. Department of Energy.

---

\*Permanent address: Department of Physics, University of Ottawa, Ottawa, Ontario, Canada K1N 6N5.

<sup>1</sup>M. Baranger, B. Giraud, S. K. Mukhopadhyay, and P. U. Sauer, Nucl. Phys. A138, 1 (1969).

<sup>2</sup>M. I. Haftel, Phys. Rev. Lett. 25, 120 (1970).

<sup>3</sup>R. D. Amado, Phys. Rev. C 2, 2439 (1970).

<sup>4</sup>W. Van Dijk and M. Ryzavy, Nucl. Phys. A159, 161 (1970).

<sup>5</sup>K. L. Kowalski, J. E. Monahan, C. M. Shakin, and R. M. Thaler, Phys. Rev. C 3, 1146 (1971).

<sup>6</sup>P. U. Sauer, Nucl. Phys. A170, 497 (1971); Ann. Phys. (N.Y.) 80, 242 (1973).

<sup>7</sup>Y. E. Kim and A. Tubis, Phys. Rev. Lett. 31, 952 (1973).

<sup>8</sup>H. S. Picker, E. F. Redish, and G. J. Stephenson, Jr., Phys. Rev. C 4, 287 (1971).

<sup>9</sup>M. J. Reiner, Ann. Phys. (N.Y.) 100, 131, 149 (1976).

<sup>10</sup>M. K. Srivastava and D. W. L. Sprung, in *Advances in Nuclear Physics*, edited by M. Baranger and E. Vogt (Plenum, New York, 1975), Vol. 8.

<sup>11</sup>R. J. W. Hodgson and J. Tan, Can. J. Phys. 54, 2225

(1976).

<sup>12</sup>M. I. Sobel, J. Phys. A 1, 610 (1968).

<sup>13</sup>J. Underhill, J. Math. Phys. 11, 1409 (1970).

<sup>14</sup>B. R. Karlsson, Phys. Rev. D 6, 1662 (1972); 10, 1985 (1974).

<sup>15</sup>R. G. Newton, *Scattering Theory of Waves and Particles* (McGraw-Hill, New York, 1966).

<sup>16</sup>D. W. L. Sprung and M. K. Srivastava, Nucl. Phys. A139, 605 (1969).

<sup>17</sup>M. Abramowitz and I. A. Stegun, *Handbook of Mathematical Functions* (Dover, New York, 1970).

<sup>18</sup>M. G. Fuda and J. S. Whiting, Phys. Rev. C 8, 1255 (1973).

<sup>19</sup>M. H. MacGregor, R. A. Arndt, and R. M. Wright, Phys. Rev. 182, 1714 (1969).

<sup>20</sup>R. W. Haymaker and L. Schlessinger, in *The Padé Approximant in Theoretical Physics*, edited by G. A. Baker, Jr. and J. L. Gammel (Academic, New York, 1970).

<sup>21</sup>K. F. Chong, Y. Singh, D. W. L. Sprung, and M. K. Srivastava, Phys. Lett. B38, 132 (1972).